



# Generation of near-inertial oscillations by summer monsoon onset over the South China Sea in 1998 and 1999



Yeqiang Shu<sup>a,b</sup>, Jiayi Pan<sup>b,c,d,\*</sup>, Dongxiao Wang<sup>a</sup>, Gengxin Chen<sup>a</sup>, Lu Sun<sup>e</sup>, Jinglong Yao<sup>a</sup>

<sup>a</sup> State Key laboratory of tropical oceanography, South China Sea Institute of Oceanology, Chinese Academy of Sciences, Guangzhou 510301, PR China

<sup>b</sup> Institute of Space and Earth Information Science, The Chinese University of Hong Kong, Hong Kong, PR China

<sup>c</sup> Shenzhen Research Institute, The Chinese University of Hong Kong, Shenzhen 518057, PR China

<sup>d</sup> College of Marine Science, Nanjing University of Information Science and Technology, Nanjing, Jiangsu 210044, PR China

<sup>e</sup> South China Sea Branch, State Oceanic Administration, Guangzhou 510301, PR China

## A B S T R A C T

The summer monsoon onset over the South China Sea (SCS) is an abrupt event in May or early June every year. After the summer monsoon onset in 1998 and 1999, strong near-inertial oscillations (NIOs) in the central SCS were observed with Acoustic Doppler Current Profilers (ADCP) mooring data. The near-inertial current speed reached  $0.25 \text{ ms}^{-1}$ , comparable to that induced by tropical storms (TS) in the same area, although the wind speed ( $\sim 10 \text{ ms}^{-1}$ ) of the monsoon onset was much lower than what is typical of TSs. Further analyses suggest that the shallow mixed-layer ( $< 30 \text{ m}$ ) in spring and the abrupt change in wind speed and direction resulting from the summer monsoon onset were responsible for developing the near-inertial current. The generated NIOs could be enhanced by a warm eddy appearing during the monsoon onset in the central SCS. The strong NIOs appeared in the middle of the SCS in May when the SCS summer monsoon starts to prevail, which implies that the beginning of the SCS summer monsoon may be a vital factor for generation of the strong NIOs in May.

## 1. Introduction

Wind forcing and downward propagation of near-inertial oscillations (NIOs) induce a substantial energy flux into the ocean available for generation of turbulence and mixing (Whalen et al., 2012; Jochum et al., 2013; Jing and Wu, 2014; Jing et al., 2016). Wind generates NIOs by exciting currents in the surface mixed-layer, and the enhanced near-inertial current shear across the mixed-layer base may induce strong mixing with a subcritical bulk Richardson number, which causes the mixed-layer to deepen and cool (Price, 1981). The NIO-induced mixing increases the ocean mixed-layer depth (MLD) by up to 30%, leading to significant changes in tropical sea surface temperature and precipitation, which may affect the local climate (Jochum et al., 2013, Wei et al., 2014).

Most strong NIOs observed in the oceans are associated with storm events, caused by the rapid increase of wind speed (Sun et al., 2011a, b; Chen et al., 2013; Zheng et al., 2006; Pollard 1970; Maeda et al., 1996). The energy of near-inertial oscillations can be modulated by vertical vorticity and stratification (Kunze, 1985; Whitt and Thomas, 2013). The frequency of a NIO may be shifted from  $f$  to  $f_{eff} = f + \epsilon/2$  in a geostrophic background flow field ( $f_{eff}$  is the effective Coriolis frequency,  $f$  is the Coriolis parameter, and  $\epsilon$  is the background geostrophic

relative vorticity). Thus, it is possible that a lower resonant frequency ( $f_{eff}$ ) will lead to more wind work input because the winds are typically characterized by a red frequency spectrum, resulting in increased near-inertial energy in the negative vorticity regions. Moreover, the effective frequency of inertial waves in a negative vorticity region might be lower than that in its surrounding region, so that NIOs will be trapped in an anti-cyclonic flow (Kunze, 1985).

The South China Sea (SCS) is the largest marginal sea in the western tropical Pacific, and its circulation is controlled by the seasonally reversing monsoonal wind (Qu, 2001). Typically, the south-westerly summer monsoon is abruptly established over the southern and central SCS in May or June every year, and soon prevails over the entire SCS (Su, 2004; Kajikawa and Wang, 2012; Wang et al., 2004). Spring is the transition season for upper ocean circulation. In this period, with the combined effects of the wind forcing and the release of high potential energy developed by the winter monsoon, an anti-cyclonic circulation emerges between  $12^\circ\text{N}$  and  $16^\circ\text{N}$  in the western SCS, resulting in a warm pool (eddy) in this area (Chu et al., 1998; He et al., 2013). Moreover, because of the weak wind forcing and strong surface heating in spring, a thin mixed-layer may appear in the central SCS (Qu, 2001). After the summer monsoon onset, the mixed-layer abruptly deepens and the warm pool disappears (Qu, 2001; Zeng et al.,

\* Corresponding author at: Institute of Space and Earth Information Science, The Chinese University of Hong Kong, Hong Kong, PR China  
E-mail address: [panj@cuhk.edu.hk](mailto:panj@cuhk.edu.hk) (J. Pan).

2009).

The SCS has frequent typhoons and tropical storm events with an average frequency of 15 events per year (Sun et al., 2011b; Xu et al., 2013). Previous investigations indicated that intensified NIOs in the SCS are usually generated by strong wind forcing of typhoons or storms (Chu et al., 2000; Sun et al., 2011a; Liu et al., 2011; Chen et al., 2013; Guan et al., 2014; Yang et al., 2015). The maximum wind speed of the SCS summer monsoon does not exceed  $12 \text{ ms}^{-1}$ , which is much lower than that of typhoons or storms. In this paper, we present observations of intensified NIOs that were closely associated with the SCS summer monsoon onset, using ADCP mooring data in two different years. The results of this study may enhance our understanding of the NIO generation mechanism, and provide a new perspective in interpreting abrupt sea surface cooling and mixed-layer deepening after the summer monsoon onset in the central SCS. The remainder of the paper is organized as follows. In-situ observations and auxiliary data used in this study are described in Section 2, and the results and analysis are presented in Section 3. Discussion is given in Section 4, followed by the conclusion in Section 5.

## 2. Data

Three 75 kHz Acoustic Doppler Current Profilers (ADCPs) were moored at locations M1 ( $115.6^\circ\text{E}$ ,  $18.0^\circ\text{N}$ ), M2 ( $115.0^\circ\text{E}$ ,  $15.3^\circ\text{N}$ ), and M3 ( $114.4^\circ\text{E}$ ,  $13.0^\circ\text{N}$ ), where the water depths are deeper than 2000 m (Fig. 1), during the SCS Monsoon Experiment (SCSMEX) from January 1998 to October 1999. Because of instrument issues, the ADCP data at M3 were only available for the period from 9 April 1998 to 10 April 1999. The mooring ADCPs were upward-looking with a bin size of 10 m and a sampling interval of 1 h. ADCP velocity records from 20 m to 170 m are used in this study. The near-inertial horizontal velocity profiles ( $u_i$ ,  $v_i$ ) are derived from the raw ADCP velocity data by using a

band-pass filter with a frequency range of  $0.85\text{--}1.15f$  (Xie et al., 2011; Chen et al., 2013). The near-inertial kinetic energy (NIKE) for each profile is calculated by

$$NIKE = \frac{1}{2} \rho_0 (u_i^2 + v_i^2) \quad (1)$$

where  $\rho_0$  ( $=1024 \text{ kg m}^{-3}$ ) is the reference density of sea water.

Sea surface winds were also observed at the three mooring stations with an interval of 10 min. Unfortunately, the anemometers failed to record wind data at M1 and M2 in the study period, and wind observations were only available at M3 from 13 April to 5 June 1998. The cross-calibrated, multi-platform (CCMP) surface wind dataset is used in this study (Atlas et al., 1996), which is available on the web ([https://podaac.jpl.nasa.gov/Cross-Calibrated\\_Multi-Platform\\_OceanSurfaceWindVectorAnalyses](https://podaac.jpl.nasa.gov/Cross-Calibrated_Multi-Platform_OceanSurfaceWindVectorAnalyses)). This dataset combines satellite winds derived from the Special Sensor Microwave Imager (SSM/I), Advanced Microwave Scanning Radiometer – Earth Observing System (AMSRE), Tropical Rainfall Measuring Mission Microwave Imager (TRMM TMI), Quikscat, and other missions, with a spatial resolution of 25 km. Level 3.0 products contain wind data sampled every 6 h, and Level 3.5 datasets are derived from the temporal average of Level 3.0 products over 5 days (pentad). Daily absolute dynamic topography (ADT), sea level anomaly (SLA), surface geostrophic velocities, and surface geostrophic velocity anomaly are obtained from AVISO gridded dataset products (<ftp://ftp.aviso.altimetry.fr>). The global  $1/12^\circ$  reanalysis product of the Hybrid Coordinate Ocean Model and the Navy Coupled Ocean Data Assimilation (HYCOM+NCODA; GLBu0.08) with 33 vertical levels from surface to 5500 m depth is used to provide a background field for the ray tracing analysis (Bleck, 2002).

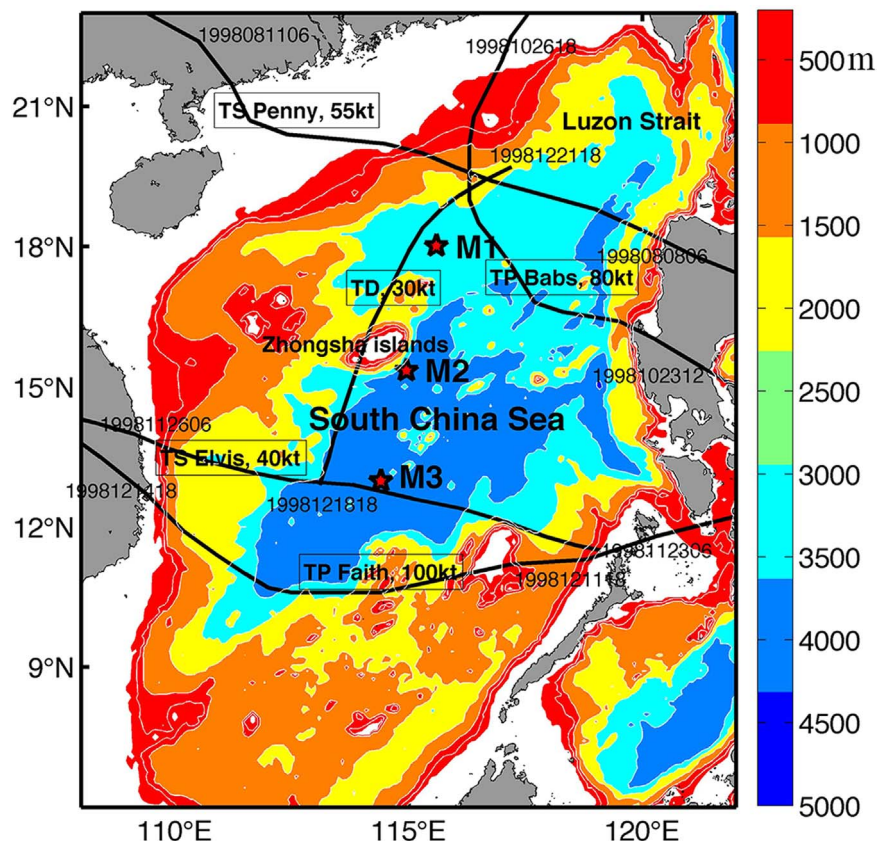


Fig. 1. The bathymetry of the SCS, where the water depth less than 200 m is blanked (white). M1, M2 and M3 are the mooring sites and the solid lines show the paths of typhoons (TP), tropical storms (TS), and tropical depressions (TD) that influenced the 3 mooring areas.

Download English Version:

<https://daneshyari.com/en/article/4534365>

Download Persian Version:

<https://daneshyari.com/article/4534365>

[Daneshyari.com](https://daneshyari.com)